Remarks on the room temperature impurity band conduction in heavily Al+ implanted 4H-SiC

Original
Remarks on the room temperature impurity band conduction in heavily Al+ implanted 4H-SiC / Parisini, Antonella; Gorni, Marco; Nath, A.; Belsito, L.; Rao, Mulpuri V.; Nipoti, R.. - In: JOURNAL OF APPLIED PHYSICS. - ISSN 0021-8979. - 118:3(2015), p. 035101. [10.1063/1.4926751]

Availability:
This version is available at: 11381/2796850 since: 2021-10-07T09:40:44Z

Publisher:
American Institute of Physics Inc.

Published
DOI:10.1063/1.4926751

AUTHOR QUERY FORM

AIP Publishing

Journal: J. Appl. Phys.

Article Number: 022528JAP

Please provide your responses and any corrections by annotating this PDF and uploading it according to the instructions provided in the proof notification email.

Dear Author,

Below are the queries associated with your article; please answer all of these queries before sending the proof back to AIP.
Please indicate the following:
Figures that are to appear as color online only (i.e., Figs. 1, 2, 3) ______________________ (this is a free service).
Figures that are to appear as color online and color in print______________________ (a fee of $325 per figure will apply).

Article checklist: In order to ensure greater accuracy, please check the following and make all necessary corrections before returning your proof.

1. Is the title of your article accurate and spelled correctly?
2. Please check affiliations including spelling, completeness, and correct linking to authors.
3. Did you remember to include acknowledgment of funding, if required, and is it accurate?

Location in article	**Query / Remark: click on the Q link to navigate to the appropriate spot in the proof. There, insert your comments as a PDF annotation.**
AQ1	Please check that the author names are in the proper order and spelled correctly. Also, please ensure that each author's given and surnames have been correctly identified (given names are highlighted in red and surnames appear in blue).
AQ2	We were unable to locate a digital object identifier (doi) for Ref(s) 13 and 34. Please verify and correct author names and journal details (journal title, volume number, page number, and year) as needed and provide the doi. If a doi is not av[illegible], no other information is needed from you. For additional information on doi's, please select this link: http://www.doi.org/.

Thank you for your assistance.

JOURNAL OF APPLIED PHYSICS **118**, 000000 (2015)

Remarks on the room temperature impurity band conduction in heavily Al^+ implanted 4H-SiC

A. Parisini,[1] M. Gorni,[1] A. Nath,[2] L. Belsito,[3] Mulpuri V. Rao,[2] and R. Nipoti[3]
[1]*CNISM-Dipartimento di Fisica e Scienze della Terra, Università di Parma, Viale G.P. Usberti 7/A, I-43124 Parma, Italy*
[2]*Department of Electrical and Computer Engineering, George Mason University, 4400 University Dr., Fairfax, Virginia 22030, USA*
[3]*CNR-IMM of Bologna, via Gobetti 101, I-40129 Bologna, Italy*

(Received 6 February 2015; accepted 1 July 2015; published online xx xx xxxx)

The processing parameters which favour the onset of an impurity band conduction around room temperature with a contemporaneous elevated p-type conductivity in Al^+ implanted 4H-SiC are highlighted by comparing original and literature results. In the examined cases, Al is implanted at 300–400 °C, in concentrations from below to above the Al solubility limit in 4H-SiC ($2 \times 10^{20}\,cm^{-3}$) and post implantation annealing temperature is $\geq$1950 °C. Transport measurements feature the onset of an impurity band conduction, appearing at increasing temperature for increasing Al implant dose, until this transport mechanism is enabled around room temperature. This condition appears suitable to guarantee a thermal stability of the electrical properties. In this study, the heaviest doped and less resistive samples (Al implanted concentration of $5 \times 10^{20}\,cm^{-3}$ and resistivity of about $2 \times 10^{-2}\ \Omega\,cm$) show a carrier density above the Al solubility limit, which is consistent with at least a 50% electrical activation for a 15% compensation. The model of Miller and Abrahams well describes the resistivity data of the lower doped sample, whereas a deviation from the behaviour predicted by such a model is observed in the higher doped specimens, consistent with the occurrence of a variable range hopping at low temperature. *© 2015 AIP Publishing LLC.* [http://dx.doi.org/10.1063/1.4926751]

INTRODUCTION

Ion implantation is the most used technology for obtaining planar selective area doping and impurity doping concentration far above the solid solubility limit in semiconductor materials for electronic device applications and for fundamental studies. Aluminum (Al) is the preferred acceptor doping species in SiC when very low p-type resistivity values are desired. To the best of the authors' knowledge, and only for demonstration purposes, the maximum implanted Al concentration in the p-type emitters of SiC p-i-n diodes has been $1.5 \times 10^{20}\,cm^{-3}$, see, for example, Refs. 1–3. In general, an increase of the semiconductor doping is desired in the device contact areas for reducing the contact resistance.

The state of the art on the electrical activation of implanted Al in 4H-SiC is hereafter resumed. For a given implanted Al concentration, the p-type doping increases with the increase of the post implantation annealing temperature, while for a fixed post implantation annealing temperature, the p-type doping increases with increasing implanted Al concentration. Maximum doping values have been obtained for 1950–2100 °C annealing with conventional[4,5] and microwave heating.[2,3] Minimum room temperature (RT) resistivity values of few $10^{-2}\ \Omega\,cm$, which are good for sheet resistance values $<10^4\ \Omega/\square$, have been obtained by implanted Al concentrations above the solubility limit of $2 \times 10^{20}\,cm^{-3}$,[6] and post implantation annealing temperatures $\geq$1950 °C.[4,5,7] The characterization of the hole transport in such low p-type resistivity Al implanted 4H-SiC materials allow us to hypothesize that implanted Al concentrations above $1.5 \times 10^{20}\,cm^{-3}$ could be used for the fabrication of highly conductive p-type paths in high temperature SiC sensors, or for designing new current collection geometries in SiC power devices. In fact, the temperature dependence of the p-type resistivity in such SiC materials features a weak temperature dependence associated to the formation of an impurity band (IB) conduction around room temperature,[2–4,8,9] which guarantee p-type SiC materials of almost stable transport features in a wide large temperature range around RT. It is worthwhile to remember that for dopant concentration below the $10^{20}\,cm^{-3}$ decade, the high thermal ionization energy of every dopant species in SiC is responsible of a strong temperature dependence of the SiC transport properties due to carrier freeze-out effects, see, for example, Refs. 10 and 11.

The aim of this article is to highlight the identification of the processing parameters which favour the onset of an impurity band conduction around room temperature joined to an elevated p-type conductivity in Al^+ implanted 4H-SiC. Both original and literature data are used for this purpose. Moreover, details on the transport data that support the identification of the IB transport mechanism in samples of different Al implant concentrations are discussed, by claiming the role of such a mechanism in obtaining very low resistivity values and a carrier density that are nearly temperature independent around RT. For one of the heavier doped samples, the consistency of the low temperature conductivity data with the Mott law was evidenced, suggesting the onset of a variable range hopping transport at low temperature.

SAMPLE PROCESSING AND MEASUREMENTS

The discussion of the transport properties of Al^+ heavily implanted 4H-SiC samples takes off from two widely recognized observations: (i) the increase of the post implantation annealing temperature leads to a more efficient electrical activation of the implanted Al impurities[2,4,8] and (ii) the increase of the activated Al concentration shifts towards higher temperatures, the onset of a hole conduction through impurity states.[8,10]

This work, following the result (i), takes into account only samples annealed at the maximum reachable temperatures of 1950 °C and 2000 °C by an inductively heated furnace[4] and by microwave heating,[7] respectively. Moreover, to discuss benefit effects of the result (ii), samples of implant concentration above $1 \times 10^{20}\,\mathrm{cm}^{-3}$ are accounted for, in the range 1.5×10^{20}–$5 \times 10^{20}\,\mathrm{cm}^{-3}$. In fact, samples with Al implanted concentration below $1 \times 10^{20}\,\mathrm{cm}^{-3}$, although submitted to the 1950 °C–2000 °C thermal treatments, exhibit a significant carrier freeze-out into impurities in a wide range of temperatures, where an electrical transport in valence band states (VB) is recognizable.[10] Features of an IB transport appear, in these samples, only by decreasing enough the temperature of measurement. The use of implanted Al concentrations above $1 \times 10^{20}\,\mathrm{cm}^{-3}$ and 1950 °C–2000 °C annealing has the effect to enhance the acceptor density, to shift the onset of the impurity band conduction towards RT and to avoid a temperature region dominated by carrier freeze-out. This condition has been effectively seen for Al implanted concentrations $\geq 3 \times 10^{20}\,\mathrm{cm}^{-3}$.[4] It is worthwhile to notice that such a density is higher than the Al solubility limit in 4H-SiC at 2000 °C, $2 \times 10^{20}\,\mathrm{cm}^{-3}$.[6]

The samples here investigated are in part a selection from previous studies and in part new processed specimens, all that with the purpose to obtain an homogeneous set of identical Al^{+} implanted 4H-SiC with 1950 °C–2000 °C post implantation annealing obtained by the two mentioned heating methods, conventional and microwave. Possible effects of different implant temperatures 300 °C and 400 °C were also inquired. Table I summarizes the sample set of this study together with their processing parameters, which are detailed in the following.

High purity semi-insulating, 8° off-axis ⟨0001⟩ 4H-SiC wafers were Al^{+} implanted with different energy and dose values to obtain almost box shaped Al depth profiles next to the wafer surface. A Tandentron 1.7 MV accelerator (High Voltage Engineering Europa B.V.) and 3 inches hot holder for sample mounting and heating were used. During implantation, the SiC samples were covered by a thick $\mathrm{SiO_2}$ film and kept at 300 °C or at 400 °C. More precisely, samples used for previous studies were implanted at 400 °C, while the original samples of this study have been implanted at 300 °C. Implantation schedules were decided by using SRIM2008 simulations[12] and verified by Secondary Ion Mass Spectroscopy (SIMS) on few samples. Homogeneous Al concentrations of 1.5×10^{20}, 3×10^{20}, and $5 \times 10^{20}\,\mathrm{cm}^{-3}$ were obtained across a thickness of about 400 nm. The implanted wafers were diced into pieces of 5 mm × 5 mm for facilitating van der Pauw (vdP) Hall measurements. These pieces were annealed at 1950 °C/5 min in a conventional inductively heated furnace ("conventional annealing" CA) or at 2000 °C/30 s in a microwave heating system ("microwave annealing" MWA). Details about these CA and MWA systems and their characteristic temperature versus time cycles are provided in Refs. 2, 7, 13, and 14. During CA and MWA, the implanted sample surface was protected by a carbon film (C-cap), which was obtained by a 900 °C/2 min pyrolysis in forming gas of a 2–4 μm thick resist film.[15] Before the spinning of the resist film, the SiC native oxide was etched away in a hydrofluoric acid bath and samples were dried in nitrogen at 110 °C for 30 min. After CA and MWA, C-cap was removed by 850 °C/15 min dry oxidation. Root mean square (rms) surface roughness after C-cap removal was measured by Atomic Force Microscopy in the tapping mode on a few samples and found to be in the range of 0.5–4.7 nm.[5]

It is widely accepted that the implanted Al does not diffuse during post implantation annealing.[9,16] This has been assumed true for all the samples of this study, which is an approximation. Such an approximation is corroborated by the fact that the measured Hall hole density always increases with the implanted Al concentration, even when this latter increases above the solubility value. Moreover, Hall hole densities overcoming the Al solubility value are effectively measured as it was shown in previous reports[2–5] and will be recalled here in the "Results and Discussion" section.

Square van der Pauw (vdP) devices have been obtained by fabricating triangular ohmic contacts on the four corners of each 5 mm × 5 mm annealed samples. For ohmic contacts, sputtered Ti(80 nm)/Al(2% Si, 350 nm) films alloyed at 1000 °C for 2 min in vacuum have been used. Due to the non-negligible dimensions of the contacts compared to the device size, correction factors have been applied to the results of electrical measurements as suggested in Ref. 17. In

TABLE I. Process parameters of the Al^{+} implanted p-type 4H-SiC samples of this study. From left to right, the column content is: sample label with, if the case, citation of previous articles where the same sample has been used, simulated implanted Al concentration by SRIM2008,[12] implantation temperature, measured as-implanted Al concentration by SIMS, post implantation annealing type (CA and MWA) with temperature and time, RT Hall hole density, and RT resistivity.

Sample	Nominal (SRIM2008) implanted Al density (cm^{-3})	Implant temp. (°C)	Measured (SIMS) implanted Al density (cm^{-3})	Post implantation annealing		RT Hall hole density (cm^{-3})	RT resistivity (Ω cm)
305g[2,3]	1.5×10^{20}	400	n. m.	MWA	2000 °C/30 s	2×10^{19}	0.067
305b	1.5×10^{20}	400	n. m.	CA	1950 °C/5 min	7×10^{18}	0.097
294c[2,3,7]	3×10^{20}	400	2.94×10^{20}	MWA	2000 °C/30 s	5×10^{19}	0.056
293a	3×10^{20}	300	2.94×10^{20}	MWA	2000 °C/30 s	5×10^{19}	0.059
293e	3×10^{20}	300	2.94×10^{20}	CA	1950 °C/5 min	5×10^{19}	0.052
296c	5×10^{20}	300	5.34×10^{20}	MWA	2000 °C/30 s	3.5×10^{20}	0.023
296e	5×10^{20}	300	5.34×10^{20}	CA	1950 °C/5 min	1.4×10^{20}	0.032

the samples of this study, such a correction resulted to increase the resistivity experimental data of a few percent (1%–4%); while more significant was the correction to the Hall voltage, which led to Hall hole values of about 10%–30% lower than the rough experimental values, depending on the contact pattern. It is worth noticing that this clarification supports the electrical quality of the samples here discussed, in fact, the correction guarantee that the reached conductivity values are not apparently enhanced by contact geometry. Four point vdP Hall measurements have been performed at the temperature range of 30–680 K and 0.8–1 T variable magnetic field. In the samples of this study, Hall hole densities from $7 \times 10^{18}\,\mathrm{cm}^{-3}$ to $1 \times 10^{21}\,\mathrm{cm}^{-3}$ have been obtained. The feasibility of the conversion of "Hall hole density" into "drift hole density," which is the true value of free carriers, through the introduction of the r_H Hall factor will be critically discussed.

RESULTS AND DISCUSSION

Figures 1(a) and 1(b) compare the temperature dependence of the Hall hole density and Hall hole mobility in two samples with identical $3 \times 10^{20}\,\mathrm{cm}^{-3}$ Al implanted concentration and identical 2000 °C/30 s MWA but different implantation temperatures: 300 °C and 400 °C, samples 294c and 293a of Table I, respectively. The curves of the two samples are identical within the experimental error. This result allows us to assume that a 100 °C reduction of the implantation temperature, from 400 °C to 300 °C, does not affect the quality of the subsequent post implantation annealing process; therefore, it allows us to compare the results of the transport measurements of all the samples of Table I, independently of their implantation temperature.

Figures 2(a) and 2(b) depict the temperature dependences of the Hall hole density and Hall mobility for all the different implanted Al concentrations of the samples of Table I and the different post implantation annealing: 1950 °C/5 min CA (closed symbols) and 2000 °C/30 s MWA (open symbols). For sake of precision, it can be added that Figs. 2(a) and 2(b) contain all the samples of Table I except 294c. The curves of Figs. 2(a) and 2(b) show that for identical implanted Al doses, the MWA samples compared to their CA counterparts show a generally higher carrier density and a correspondingly lower mobility, while keeping very similar trends of temperature dependence. The major physical difference between conventional and microwave heating may be an interaction between the microwave field and the free carriers in the implanted layer, the more the electrical activation of the implanted dopant proceeds. Such an effect could be tested if identical CA and MWA thermal cycles could be compared, but presently this is not possible because of the technical constrains of the two annealing set-ups. In this situation, the differences between the correspondent CA and MWA curves of Figs. 2(a) and 2(b) are ascribed to the 50 °C higher temperature of the MWA compared to the CA. Hereafter, the features of the curves of Figs. 2(a) and 2(b) will be discussed only with respect to the value of the implanted Al concentration.

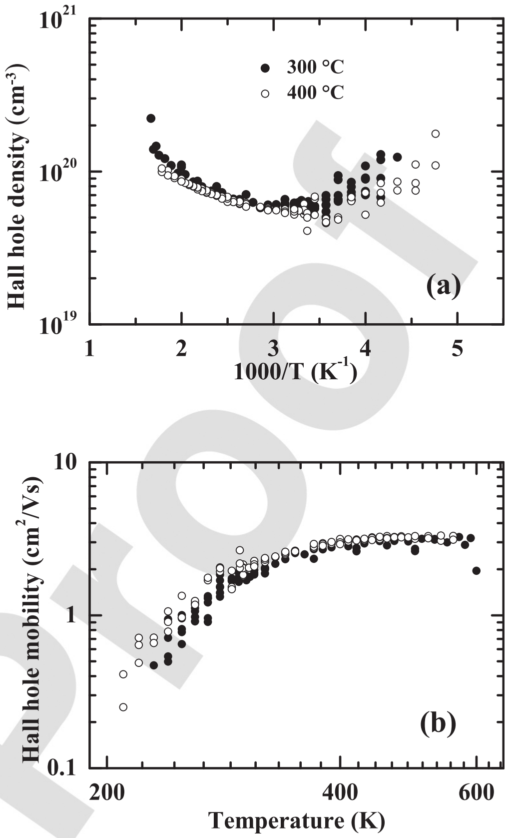

FIG. 1. Comparison of (a) the Hall hole density and (b) the Hall hole mobility for $3 \times 10^{20}\,\mathrm{cm}^{-3}$ Al$^+$ implanted and 2000 °C/30 s MWA 4H-SiC samples, which are different only for the implantation temperature: (close symbols) 300 °C and (open symbols) 400 °C. The experimental data were corrected for contact size systematic error (see text).

Only the $1.5 \times 10^{20}\,\mathrm{cm}^{-3}$ Al implanted specimens have an Arrhenius plot of the Hall hole density data where an exponential trend is observable (see Fig. 2(a)), which is typical for the carrier transport through valence band states in the hole freeze-out regime. Such a trend takes place above about 200 K and it is consistent with an acceptor thermal ionization energy of about 100 meV, in agreement with the conclusions of Ref. 10. The temperature (T) dependence of the correspondent mobility curves (see Fig. 2(b)) shows a trend almost equal to $T^{-3/2}$ that is typical of phonon scattering. This result says that the crystalline quality of these implanted and annealed 4H-SiC specimens is preserved in spite of an implanted Al concentration approaching the solubility value. Notwithstanding this, a fitting of the Hall data was not performed, because the model for transport discussed in Ref. 10 is reliable below an acceptor density of $10^{20}\,\mathrm{cm}^{-3}$. For temperatures lower than 200 K, the data of this CA sample show the hint of a minimum in the Hall density curve with the correspondent mobility data decreasing more abruptly than the typical trend expected for ionized impurity scattering, the latter having a $T^{3/2}$ temperature dependence or weaker. These features are generally recognized as due to the onset of a impurity band conduction, which prevails at low temperatures, whereas around the Hall density minimum a mixed carrier transport takes place between IB and VB states, as reviewed, e.g., by Mott in Ref. 18. The theoretical Hall density and mobility curves depicted in Ref. 10, however, show

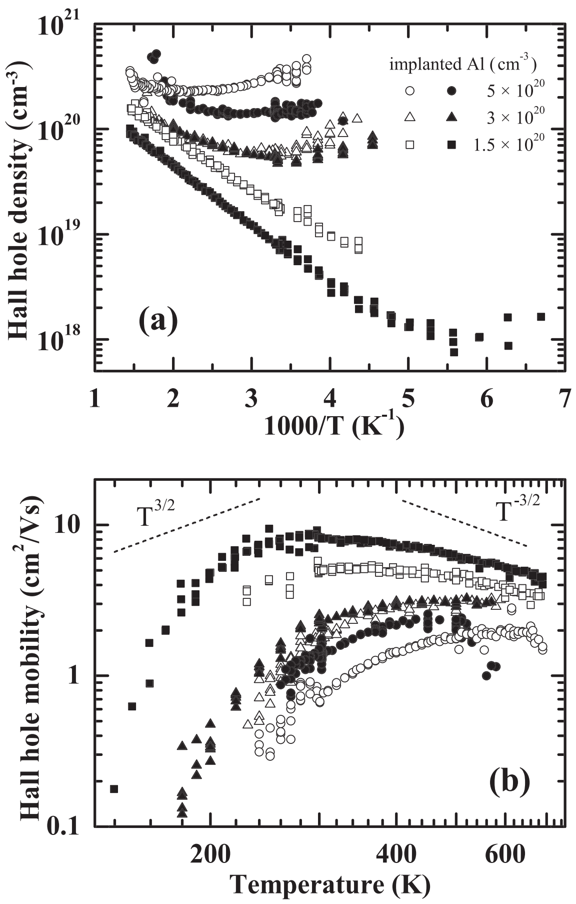

FIG. 2. Temperature dependence of: (a) the Hall hole density and (b) the Hall hole mobility of given Al implanted concentrations in 8° off-axis ⟨0001⟩ high-purity semi-insulating 4H-SiC and different post implantation annealings: CA 1950 °C/5 min (full symbols), and MWA 2000 °C/30 s (open symbols). The implanted Al concentration is shown in the inset of (a). For comparison, the trends $T^{3/2}$ and $T^{-3/2}$ for ionized impurity scattering and non-polar phonon scattering, respectively, are shown as dashed lines in (b). The experimental data were corrected for contact size systematic error (see text).

a departure from experimental data towards the low temperatures, yet before such a minimum, suggesting that the influence of the transport through localized states is effective at higher temperatures in respect to that of such a minimum. In the $1.1 \times 10^{20}\,\mathrm{cm}^{-3}$ Al implanted sample, in particular, a weak effect of the IB conduction can be presumable up to the proximity of RT.

The $3 \times 10^{20}\,\mathrm{cm}^{-3}$ and $5 \times 10^{20}\,\mathrm{cm}^{-3}$ Al implanted specimens show a weak temperature dependence of the Hall hole density values, weaker for higher implanted Al concentrations, and broad minima centred at about room temperature and above room temperature for the lower and higher implanted Al concentration, respectively (see Fig. 2(a)). The sign of the Hall coefficient was that expected for positive carriers at any temperature. The correspondent mobility values have a temperature dependence dominated by an almost flat trend at high temperature and a steep decrease with decreasing temperature, as for the $1.5 \times 10^{20}\,\mathrm{cm}^{-3}$ Al implanted samples (see Fig. 2(b)). In the light of the global trends of all the samples, the occurrence of a mixed conduction where the transport through impurity states is relevant at any temperature has been hypothesized. The possibility to observe a significant IB conduction at so high temperatures like room temperature and above is not usual and it is possible in p-type 4H-SiC, owing to the high thermal ionization energy of the Al acceptors. An IB conduction around room temperature has been previously reported in 4H-SiC for a much higher Al implanted concentration of $1.5 \times 10^{21}\,\mathrm{cm}^{-3}$, where the samples were implanted at comparable temperature than in the present study but annealed at a much lower temperature (1600 °C/10 min).[8] Major differences between the results of this study and those of Ref. 8 are a higher hole density, higher mobility, and lower resistivity values in the former. These differences can be justified by a more efficient activation of the implanted dopant in this work, thanks to the higher annealing temperatures, 1950 °C–2000 °C against 1600 °C. This result must be highlighted, because it indicates that these extreme annealing processes permit to reach a high enough acceptor density to induce a significant IB conduction around RT at lower implant dose in respect to Ref. 8, without detrimental effects on the mobility, which, on the contrary, is favoured probably by a lower amount of lattice disorder.

The estimation of the electrical activation (the fraction between dopant density in substitution positions and implanted dopant density) of a given post-implantation annealing process is generally possible if the transport of carriers takes place in the extended state band (VB), although the need of the Hall factor correction, r_H, which converts Hall into drift data, to avoid systematic inaccuracies, must be highlighted. In Ref. 10, it has been shown that this evaluation is reliable by fitting the data in the relaxation time approximation (RTA), till a maximum Al implanted concentration of $1.12 \times 10^{20}\,\mathrm{cm}^{-3}$, by adopting an empirically obtained Hall factor for Al doped p-type 4H-SiC.[19] In such p-type samples, the Hall factor must account for the occupancy of both the heavy and light hole valence bands and their anisotropy. In fact, in the case of two parallel channels "1" and "2," r_H takes the form

$$r_H = (p_1 + p_2)e\frac{\sigma_1\mu_{1H} + \sigma_2\mu_{2H}}{(\sigma_1 + \sigma_2)^2}. \qquad (1)$$

In Eq. (1), p_i, σ_i, and μ_{iH} are the hole density, the conductivity, and the Hall mobility in the i^{th} conduction channel ($i = 1, 2$); e is the electron charge. In the same channel of transport, the Hall and *drift* (*true*) mobility, μ_{iH} and μ_i, respectively, are generally different. The ratio μ_{iH}/μ_i is the *intra-valley* Hall factor, r_{Hi}, which for a transport into a band of extended states (i.e., the states of the valence or conduction band) can be computed in the frame of the RTA. In this framework, r_{Hi} is defined as the product of the scattering factor $r_{Si} = \langle\tau_i^2\rangle/\langle\tau_i\rangle^2$ with the mass anisotropy factor r_{Ai}, that is, $r_{Hi} = r_{Si}r_{Ai}$ [Ref. 20 and references therein]. The scattering factor r_{Si} accounts for the kinetic energy distribution of free carriers within a given band (for non-monokinetic carriers), whereas the mass anisotropy factor r_{Ai} is a correction to r_{Si} due to a possible anisotropy of such a band. For p-type 4H-SiC, Eq. (1) has been used in Refs. 10 and 20–22, with some different assumptions, to describe the hole transport through the two parallel channels of the heavy and the light hole valence bands for acceptor concentration in the range 2×10^{15}–$1 \times 10^{20}\,\mathrm{cm}^{-3}$.

When a transport through an impurity band is added in parallel to the transport through extended states, which, in this study, is the case for the $3 \times 10^{20}\,\mathrm{cm}^{-3}$ and $5 \times 10^{20}\,\mathrm{cm}^{-3}$ samples over the whole temperature range of measurements, it is hard to apply Eq. (1) to obtain the Hall factor. In fact, the interpretation of the Hall coefficient R_H as a quantity simply related to the reverse of the carrier density (*normal* Hall effect) becomes doubtful for an impurity band conduction; the sign of the Hall voltage could even to be inverted in this regime.[18,23,24] In this contest, the Hall factor r_H could empirically account for any deviation of the Hall coefficient R_H from its *normal* meaning, but it could take values not simply predictable. In any case, for the conduction through localized states, the Hall factor r_H loses its usual meaning because the hopping transport can be described through a thermally activated hopping probability, which cannot be calculated in terms of an energy dependent relaxation time. On the other hand, Mott suggested that in IB conduction, around the transition to metal, if the Hall coefficient does not have an abnormal sign, its value is not far from the value expected for the carrier density.[18] However, the conversion of the Hall values of Fig. 2(a) for the heaviest doped samples in *drift* ones is not reliable and thus neither the correspondent acceptor density can be simply estimated. In spite of this conclusion, the following qualitative analysis on the curves of Fig. 2(a) can be performed.

Although none of the curves of Fig. 2(a) shows carrier exhaustion, the Hall hole density data of the samples with the higher Al implanted concentration of $5 \times 10^{20}\,\mathrm{cm}^{-3}$ could be used for a rough estimation of the maximum net acceptor density (acceptor density minus compensating impurity density). In fact, the net acceptor density can be considered at least equal to the experimental Hall hole density measured at higher temperature, where the transport through extended states is expected to be dominant and then the *intra-valley* r_H factor of Ref. 19 can be tentatively assumed to correct the Hall data. The 2000 °C/30 s MWA sample shows a maximum Hall density at the highest temperature of $3.5 \times 10^{20}\,\mathrm{cm}^{-3}$, which, if reduced of a r_H factor of about 0.6, is consistent with a net acceptor value of about $2.2 \times 10^{20}\,\mathrm{cm}^{-3}$. This density may correspond to a 100% electrical activation for about a 50% compensation, or to a more than 50% electrical activation for a 15% compensation. The latter hypothesis seems to be more reasonable in the light of the electrical activation and compensation which have been obtained for Al implanted 4H-SiC samples in the range 5×10^{19}–$1.5 \times 10^{20}\,\mathrm{cm}^{-3}$ and 1950 °C/5 min CA: 70% and 10%–13%, respectively.[10]

A confirmation of the occurrence of a transport through localized states can be inferred from the study of the temperature dependence of the implanted material sheet resistance or the material resistivity, which is the measured sheet resistance multiplied by implanted layer thickness. No correction to the implanted thickness needed to be accounted for Ref. 25, at any temperature, the surface/interface depletion of the layer being negligible (however, such a correction would have the effect to reduce further the resistivity data). Sheet resistance has been measured in absence of magnetic field, even if none magneto-resistance effect has ever been detected for the samples of this study. Figs. 3(a) and 3(b) show the Arrhenius plots of the resistivity of all the samples of this study, the same data are plotted on two different temperature windows in order to clearly visualize the resistivity temperature dependence around and above RT in the case of Fig. 3(a), and even below RT in the case of Fig. 3(b). It is evident that, for each sample, sheet resistance measurements were performed until lower temperatures than those of Hall measurements, whose scattering increases more and more with the sample cooling. Such a scattering is due to the very low values of the Hall potential at such very high carrier densities, while the contacts preserve their ohmic behavior up to 10 K and the current can flow at any temperature through the implanted layers because the carrier density remains high thanks to the IB conduction. The sheet resistance, which increases with decreasing temperature, is measurable until the voltage drop at the vdP contacts does not overpasses the voltage limit of the used instrument set-up. The resistivity data, then obtained, show some general trends (see Figs. 3(a) and 3(b)), which confirm previously published results, see, as an example, Ref. 8. In particular, all the samples of this

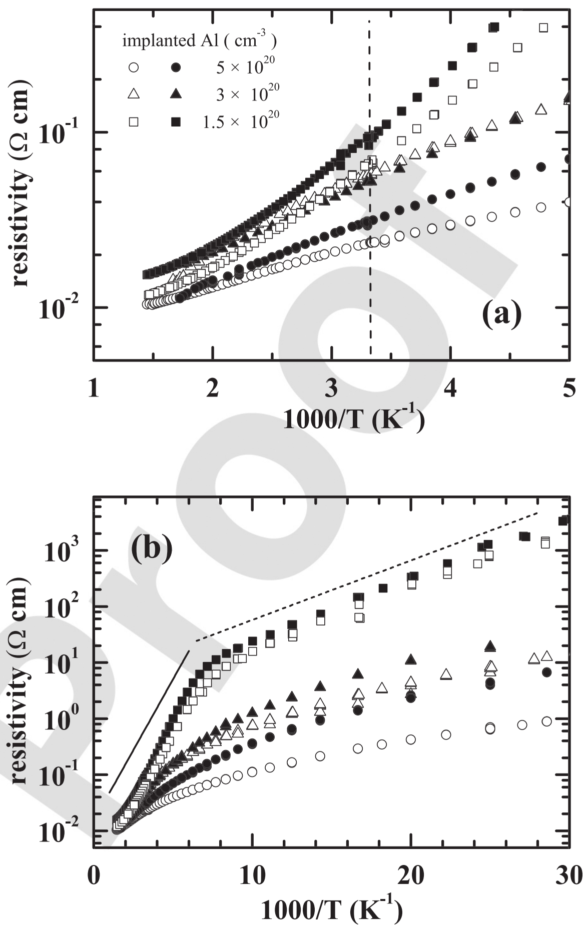

FIG. 3. Arrhenius plot of the resistivity data for all the sample of this study: (a) aro[illegible]d above RT, (b) over the whole range of ~~temperature of measurements~~. The implanted Al concentrations are shown in the inset of (a). Open and full symbols refer to MWA and CA samples, respectively. The vertical dashed line of (a) corresponds to room temperature. Dashed and continuous lines in (b) show the exponential trends for 20 meV and 100 meV activation energies, respectively. The experimental data were corrected for contact size systematic error (see text).

study have resistivity values that decrease with increasing temperature as expected for a semiconductor material. This result is consistent with the published range of 6.4×10^{20}–$8.7\times10^{20}\,\mathrm{cm}^{-3}$ Al concentrations for the occurring of the metal to insulator transition (MIT), which has been observed in liquid phase epitaxial growth 4H-SiC materials.[26] In fact, in this study, the maximum value of Al implanted concentration is $5\times10^{20}\,\mathrm{cm}^{-3}$. It should also be noted that implanted materials are expected to contain more crystal disorders than the epitaxial ones. For elevated doping densities, the presence of crystal disorder could favor the persistence of a hopping conduction by inhibiting the MIT. Concerning the comparison of the two annealing methods, Figs. 3(a) and 3(b) show that for identical implanted Al concentration; the resistivity of the MWA specimen is generally lower than that of the ~~CA, one~~ which is attributed to a more efficient electrical activation by the MWA method because of its higher temperature. Finally, Figs. 3(a) and 3(b) show that the resistivity values decrease for increasing implanted Al concentration. The minimum RT resistivity obtained in the Al^+ 4H-SiC material of this study is $2.3\times10^{-2}\ \Omega$ cm for the $5\times10^{20}\,\mathrm{cm}^{-3}$ implanted Al concentration and 2000 °C/30 s MWA. This result agrees with the conclusions of Heera *et al.*,[27] who calculated the values of minimum resistivity as a function of the acceptor density expected for hole transport through extended states in the ideal case of null compensation and predicted that resistivity data lower than such minimum values could be obtained only by achieving a transport through an impurity band. In particular, they[27] computed a resistivity of $7\times10^{-2}\ \Omega$ cm for hole transport in valence band with $5\times10^{20}\,\mathrm{cm}^{-3}$ Al concentration.

The transition between a carrier conduction through band states to IB conduction is particularly evident in the $1.5\times10^{20}\,\mathrm{cm}^{-3}$ Al implanted samples. In these samples, both the regimes are clearly visible in a wide temperature range, despite some mixed conduction effects in between. Around and above room temperature (see Fig. 3(a)), the Arrhenius plots of the p-type resistivity of these samples show a clear exponential trend with thermal activation energy of about 100 meV, which agrees with that obtained from the data of Fig. 2(a). By decreasing temperature (see the curves of Fig. 3(b)), the resistivity Arrhenius plots of the $1.5\times10^{20}\,\mathrm{cm}^{-3}$ samples show a transition from the high temperature exponential trend to another exponential trend of much lower activation energy, about 20 meV, towards lower temperatures. This transition takes place in a narrow temperature window around about 200 K. Such a broken-straight line behavior can be commented according to the pioneering model of Miller and Abrahams.[28] This model describes the temperature dependence of the conductivity in semiconductor materials $\sigma(T)$ as the sum of three thermally activated conduction mechanisms: σ_1, σ_2, and σ_3, due to the trans[illegible] into extended states (valence or conduction band), ~~hopping~~ [illegible] to the higher impurity Hubbard band, and ~~between~~ impurity states, respectively

$$\sigma(T) = \sigma_1 + \sigma_2 + \sigma_3$$
$$= \sigma_{01}e^{-\epsilon_1/K_BT} + \sigma_{02}e^{-\epsilon_2/K_BT} + \sigma_{03}e^{-\epsilon_3/K_BT}. \quad (2)$$

In Eq. (2), ϵ_1, ϵ_2, and ϵ_3 are the thermal activation of the three transport mechanisms, respectively, and K_B is the Boltzmann constant. Generally, the σ_1 and σ_3 contributions extend over wide temperature windows, while the possibility to detect the σ_2 contribution is restricted to a narrow temperature range in between those of σ_1 and σ_3, and limited to intermediate doping conditions even depending on the compensation ratio.[29,30] A linear trend appearing in the low temperature Arrhenius plot of the resistivity is, in the most of the cases, attributable to a transport through a hopping mechanism between an occupied dopant atom to a nearest unoccupied one. Therefore, in the case of the $1.5\times10^{20}\,\mathrm{cm}^{-3}$ sample, the ≈20 meV activated transport was attributed to a hopping conduction between nearest Al acceptors. The model of this hopping mechanism predicts a thermal activation energy ϵ_3 dependent on compensation and doping level.[28–31]

A departure from the behavior of the $1.5\times10^{20}\,\mathrm{cm}^{-3}$ sample is observed in the data of the heavier doped samples, of implanted Al concentration $\geq 3\times10^{20}\,\mathrm{cm}^{-3}$, whose resistivity Arrhenius plots do not evidence any reliable straight trend in the whole temperature range if accurately analyzed; therefore, in their low temperature conductivity data, neither the σ_2 nor the σ_3 contributions can be recognized. A similar behavior has been not claimed by Heera *et al.*,[8] who interpreted the resistivity data of all their samples, none of which displayed the maximum doping level here reached, in terms of the Miller and Abrahams model.

The ensemble of the results of this study on Al^+ implanted 4H-SiC materials, instead, agrees with the experimental results of Müller *et al.*[32] on Al doped 6H-SiC bulk materials. In fact, these authors performed temperature dependent Hall effect measurements on samples with specific resistivity in the ran[illegible]1–8 Ω cm. In all these samples, indications for ~~impurity conduction~~ at low temperatures have been found with the following major difference. In the lower doped samples ($\rho > 0.2\ \Omega$ cm), a sharp transition between impurity and valence band conduction transport was visible in the temperature dependence of specific resistivity, charge carrier concentration, and mobility. In highly doped samples ($\rho < 0.2\ \Omega$ cm), the same transition was no longer confined to a small temperature range and it was much less abrupt. Müller *et al.*[32] concluded that in their heavily Al doped bulk 6H-SiC, the impurity conduction was present at high temperatures so that at least two competing transport mechanisms took place simultaneously. In the Al^+ implanted 4H-SiC samples of this study, a resistivity one order of magnitude lower has been achieved and the phenomenon is much more evident.

The fact that no clear exponential trend can be recognized in our samples could be justified, at least partially, in terms of mixed conduction effects, involving extended and localized states. However, with the aim to confirm in our samples the departure from the nearly piecewise linear behavior predicted by Eq. (2) for the Arrhenius plot of the conductivity data, the $\log_{10}[d\ln(\sigma)/d\ln(T)]$ function was numerically calculated from the conductivity of our samples, following the approach of, among others, Ref. 33. The slope p of the resulting data, plotted as a function of $\log_{10}[T]$, is expected to equal the value -1 when the conductivity exhibits a thermally activated behavior, like $\sigma_0 e^{-\epsilon/K_B T}$. Similarly, the sum of two (or more) thermally activated behaviors, as they are in Eq. (2), must lead to two (or more) linear traits with slope $p = -1$. This is sketched in the inset of Fig. 4(a), which plots in double logarithmic scale, the calculation of $d\ln(\sigma_{teo})/d\ln(T)$ performed on a test function $\sigma_{teo} = \sigma_{01} e^{-\epsilon_1/K_B T} + \sigma_{03} e^{-\epsilon_3/K_B T}$. The expectation of a $p = -1$ slope is qualitatively fulfilled for the low temperature data of the $1.5 \times 10^{20}\,\mathrm{cm}^{-3}$ Al implanted samples, as it appears in Fig. 4(a) for sample 305b of Table I, for which the hypothesis of thermally activated hopping conduction between localized states at low temperature is confirmed. At the same time, Fig. 4(a) shows that the higher temperature conductivity data of sample 305b, which should correspond to valence band state transport, agree with a p value a little higher than unity. This is consistent with non-exact linearity of the high temperature data in the Arrhenius plot of Fig. 3(b), due to the effective temperature dependence of the total VB density of the states and of the carrier mobility. A transition region exists between these two different transport regimes, indicated by an arrow in Fig. 4(a), consistent with the trend of the theoretical example reported in the inset of the same figure. Fig. 4(b) reports the result of the same type of analysis of Fig. 4(a) but for one of the $3 \times 10^{20}\,\mathrm{cm}^{-3}$ Al implanted samples, more precisely sample 293e of Table I: notwithstanding the scattering of the data; at low temperature, their slope undoubtedly departs from the value $p = -1$, which, however, seems to be a slope occurring just around RT. This preliminary result roughly suggests the appearance of a transport mechanism at lower temperatures different from the nearest neighbor hopping, consistent with the Mott law $\sigma = \sigma_0 e^{-\epsilon/K_B T^{0.25}}$. A nearest neighbor hopping transport, instead, could not be excluded around RT. The Mott law has been derived in the treatment of the variable range hopping, which is a transport mechanism effectively expected in proximity of the MIT transition,[31] previously never pointed out in p-type 4H-SiC. However, the given Mott law seems not to fully explain the temperature dependence of all the heaviest doped samples here discussed~~;~~ although for all them, the departure of the conductivity from Eq. (2) is confirmed.

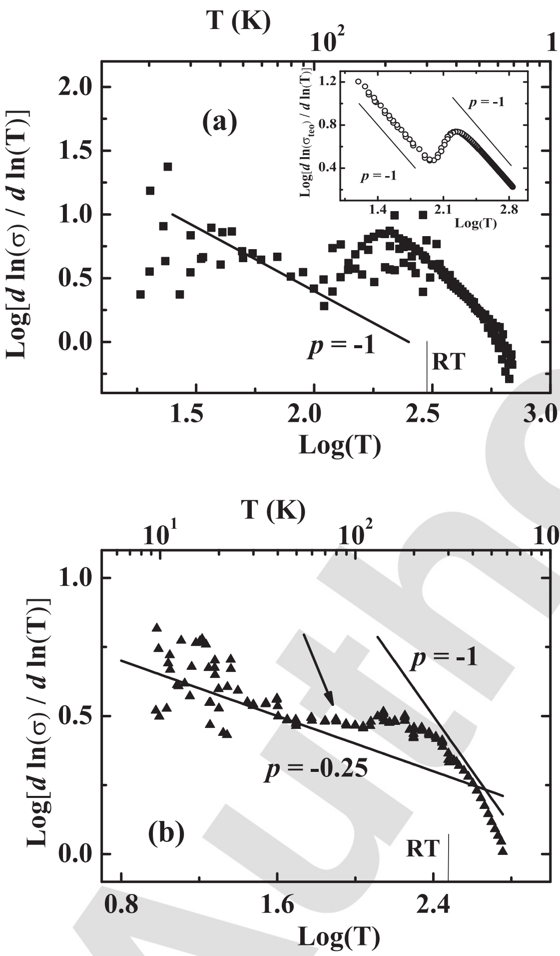

FIG. 4. Plot of $\log_{10}[d\ln(\sigma)/d\ln(T)]$ versus $\log_{10}[T]$ for the measured σ of (a) sample 305b of Table I (Al implanted density of $1.5 \times 10^{20}\,\mathrm{cm}^{-3}$, CA 1950 °C/5 min; full square), (b) ~~for~~ sample 293e of Table I (Al implanted density of $3 \times 10^{20}\,\mathrm{cm}^{-3}$, CA 1950 °C/5 min; full triangle). Inset of Figure (a): $\log_{10}[d\ln(\sigma_{teo})/d\ln(T)]$ versus $\log_{10}[T]$ for the test function $\sigma_{teo} = 300 \exp(-0.1/K_B T) + 0.45 \exp(-0.021/K_B T)$, which roughly approximate the conductivity data of the sample of Figure (a) like the sum of two thermally activated contributions (see Eq. (2)). For guiding the eyes, straight lines with slope either -1 or -0.25, are also shown in the figures. Moreover, for reference, a vertical thin line is placed at about RT and the linear temperature scale is shown on the top axis, while arrows are drawn to point the transition region between two different transport regimes.

CONCLUSIONS

In conclusion, the unusual electrical properties of the $\geq 3 \times 10^{20}\,\mathrm{cm}^{-3}$ Al implanted 4H-SiC ~~samples that~~ allow us to observe an IB conduction over a large temperature window just around RT associated to a low p-type 4H-SiC material ~~resistivity~~ ~~is~~ possible thanks to the simultaneous occurrence of three aspects

(1) An implanted dopant concentration above the Al solubility limit of $2 \times 10^{20}\,\mathrm{cm}^{-2}$.
(2) A very efficient electrical activation process due to the extremely high post implantation annealing temperatures of 1950 °C and 2000 °C.
(3) The high thermal ionization energy of the acceptors in p-type 4H-SiC.

A nearly temperature independent free hole density can be obtained around RT in these samples, a feature that can guarantee good thermal stability in applications where such a stability is required. Ion implantation even permits to simplify the processing steps for reaching such a condition in selected areas. Weakly T-dependent transport properties were obtained, in this work, at lower implant dose and higher electrical activation of the implanted impurities in respect to results of other authors. No significant effects due to the implant temperature variation between 300 °C and 400 °C were evidenced. In $5 \times 10^{20}\,\mathrm{cm}^{-3}$ Al implanted samples, hole density values overcoming the Al solubility limit in 4H-SiC were reached, consistent with at least a 50% electrical activation if a 15% compensation is supposed. These doping conditions lead to the lowest RT resistivity values ever reported in the literature for p-type 4H-SiC, to the best of the authors knowledge, with more favourable results in MWA samples, owing to the 50 °C higher temperature of the treatment in respect to CA. The temperature dependence of the resistivity was well explained by the model of Miller and Abrahams in the samples of carrier density lower than 3×10^{20} (here investigated and from the literature), whereas a deviation from this behaviour is observed above such a density, consistent with the occurrence of a variable range hopping transport mechanism at low temperatures.

Theory and experiments on impurity band conduction lead to conclude that such a transport mechanism takes place at higher and higher temperature with the increasing of the dopant ionization energy. SiC is certainly a good material to see this trend because of the quite deep energy level of every dopant species. Actually, SiC was the first semiconductor where transport through an impurity band was hypothesized in 1946.[34] The novelty to see an impurity band transport around room temperature in p-type SiC dates on the years 2004–2006, roughly.[8,9,32] The novelty to obtain an impurity band transport with features of interest for practical devices is shown in the present study.

ACKNOWLEDGMENTS

Authors warmly acknowledge S. Vantaggio for the contribution to low temperature Hall effect measurements. M. Bellettato, F. Bonafè, M. Sanmartin, and G. Pizzochero of the CNR-IMM-UOS of Bologna, P. De Nicola of MIST E-R s.r.l., and Y.-L. Tian of LT Technologies are acknowledged for their contribution to sample processing. This work was partially supported by the Army Research Office (ARO under Contract No. W911NF-09-1-0407) and also by DARPA through the U.S. Naval Research Laboratory Contract No. N0017310-2-C006.

[1] R. Nipoti, F. Moscatelli, and P. D. Nicola, IEEE Electron Device Lett. **34**, 966 (2013).
[2] A. Nath, V. R. Mulpuri, Y.-L. Tian, A. Parisini, and R. Nipoti, J. Electron. Mater. **43**, 843 (2014).
[3] A. Nath, A. Parisini, Y.-L. Tian, V. R. Mulpuri, and R. Nipoti, Mater. Sci. Forum **778–780**, 653 (2014).
[4] R. Nipoti, R. Scaburri, A. Hallén, and A. Parisini, J. Mater. Res. **28**, 17 (2013).
[5] R. Nipoti, A. Hallén, A. Parisini, F. Moscatelli, and S. Vantaggio, Mater. Sci. Forum **740–742**, 767 (2013).
[6] M. K. Linnarsson, U. Zimmermann, J. Wong-Leung, A. Schöner, M. S. Janson, C. Jagadish, and B. G. Svensson, Appl. Surf. Sci. **203–204**, 427 (2003).
[7] R. Nipoti, A. Nath, M. V. Rao, A. Hallen, A. Carnera, and Y. L. Tian, Appl. Phys. Express **4**, 111301 (2011).
[8] V. Heera, K. N. Madhusoodanan, W. Skorupa, C. Dubois, and H. Romanus, J. Appl. Phys. **99**, 123716 (2006).
[9] Y. Negoro, T. Kimoto, H. Matsunami, F. Schmid, and G. Pensl, J. Appl. Phys. **96**, 4916 (2004).
[10] A. Parisini and R. Nipoti, J. Appl. Phys. **114**, 243703 (2013).
[11] M. Laube, F. Schmid, G. Pensl, G. Wagner, M. Linnarsson, and M. Maier, J. Appl. Phys. **92**, 549 (2002).
[12] See http://www.srim.org/ for SRI ion implantation simulation code.
[13] Y.-L. Tian, MRS Bull. **35**, 181 (2010). AQ2
[14] H. M. Ayedh, V. Bobal, R. Nipoti, A. Hallen, and B. G. Svensson, J. Appl. Phys. **115**, 012005 (2014).
[15] R. Nipoti, F. Mancarella, R. Rizzoli, S. Zampolli, and M. Ferri, Electrochem. Solid-State Lett. **13**, H432 (2010).
[16] S. G. Sundaresan, V. R. Mulpuri, Y.-L. Tian, M. C. Ridgway, J. A. Schreifels, and J. J. Kopanski, J. Appl. Phys. **101**, 73708 (2007).
[17] R. Chwang, B. J. Smith, and C. R. Crowell, Solid-State Electron. **17**, 1217 (1974).
[18] N. F. Mott and E. A. Davis, *Electronic Processes in Non-Crystalline Materials* (Clarendon Press, Oxford, 1971), Chap. 2, p. 53; Chap. 6, p. 152.
[19] F. Schmid, M. Krieger, M. Laube, G. Pensl, and G. Wagner, in *Hall Scattering Factor for Electron and Holes in SiC in Silicon Carbide*, Recent Major Advances, edited by W. J. Choyke, H. Matsunami, and G. Pensl (Springer-Verlag, Berlin/Heidelberg, 2004), p. 517.
[20] J. D. Wiley, in *Mobility of Holes in III-V Compounds*, Semiconductor and Semimetals, edited by R. K. Willardson and A. C. Beer (Academic Press, New York, 1975), Vol. 10, p. 91.
[21] A. Koizumi, J. Suda, and T. Kimoto, J. Appl. Phys. **106**, 013716 (2009).
[22] J. Pernot, S. Contreras, and J. Camassel, J. Appl. Phys. **98**, 023706 (2005).
[23] T. Holstein, Phys. Rev. **124**, 1329 (1961).
[24] D. Emin, Philos. Mag. **35**, 1189 (1977).
[25] A. Chandra, C. E. C. Woodard, and L. F. Eastman, Solid State Electron. **22**, 645 (1979).
[26] P. Achatz, J. Pernot, C. Marcenat, J. Kacmarcik, G. Ferro, and E. Bustarret, Appl. Phys. Lett. **92**, 072103/1-3 (2008).
[27] V. Heera, D. Panknin, and W. Skorupa, Appl. Surf. Sci. **184**, 307 (2001).
[28] A. Miller and E. Abrahams, Phys. Rev. **120**, 745 (1960).
[29] E. A. Davis and W. D. Compton, Phys. Rev. **140**, A2183 (1965).
[30] H. Fritzsche and M. Cuevas, Phys. Rev. **119**, 1238 (1960).
[31] B. I. Shklovskii and A. L. Efros, *Electronic Properties of Doped Semiconductors* (Springer-Verlag, Berlin/Heidelberg, 1984), p. 74.
[32] R. Müller, U. Künecke, R. Weingärtner, M. Maier, and P. Wellmann, Phys. Status Solidi C **3**, 554 (2006).
[33] A. Y. Rogatchev and U. Mizutani, Phys. Re 1, 15550 (2000).
[34] G. Busch and H. Labhart, Helv. Phys. Acta ~~14~~, 463 (1946).